JACS
JOURNAL OF THE AMERICAN CHEMICAL SOCIETY
Article
pubs.acs.org/JACS

Enantiomerically Pure Trinuclear Helicates via Diastereoselective Self-Assembly and Characterization of Their Redox Chemistry

Christoph Gütz,[†] Rainer Hovorka,[†] Niklas Struch,[†] Jens Bunzen,[†] Georg Meyer-Eppler,[†] Zheng-Wang Qu,[‡] Stefan Grimme,*[,‡] Filip Topić,[§] Kari Rissanen,[§] Mario Cetina,[∥] Marianne Engeser,*[,†] and Arne Lützen*[,†]

[†]Kekulé-Institute of Organic Chemistry and Biochemistry, University of Bonn, Gerhard-Domagk-Str. 1, D-53121 Bonn, Germany
[‡]Mulliken Center for Theoretical Chemistry, University of Bonn, Beringstr. 4, D-53115 Bonn, Germany
[§]Department of Chemistry, University of Jyväskylä, Nanoscience Center, P.O. Box 35, 40014 Jyväskylä, Finland
[∥]Department of Applied Chemistry, Faculty of Textile Technology, University of Zagreb, Prilaz baruna Filipovića 28a, HR-10000 Zagreb, Croatia

Supporting Information

ABSTRACT: A tris(bipyridine) ligand **1** with two BINOL (BINOL = 2,2′-dihydroxy-1,1′-binaphthyl) groups has been prepared in two enantiomerically pure forms. This ligand undergoes completely diastereoselective self-assembly into D_2-symmeteric double-stranded trinuclear helicates upon coordination to copper(I) and silver(I) ions and to D_3-symmetric triple-stranded trinuclear helicates upon coordination to copper(II), zinc(II), and iron(II) ions as demonstrated by mass spectrometry, NMR and CD spectroscopy in combination with quantum chemical calculations and X-ray diffraction analysis. According to the calculations, the single diastereomers that are formed during the self-assembly process are strongly preferred compared to the next stable diastereomers. Due to this strong preference, the self-assembly of the helicates from racemic **1** proceeds in a completely narcissistic self-sorting manner with an extraordinary high degree of self-sorting that proves the power and reliability of this approach to achieve high-fidelity diastereoselective self-assembly via chiral self-sorting to get access to stereochemically well-defined nanoscaled objects. Furthermore, mass spectrometric methods including electron capture dissociation MS^n experiments could be used to elucidate the redox behavior of the copper helicates.

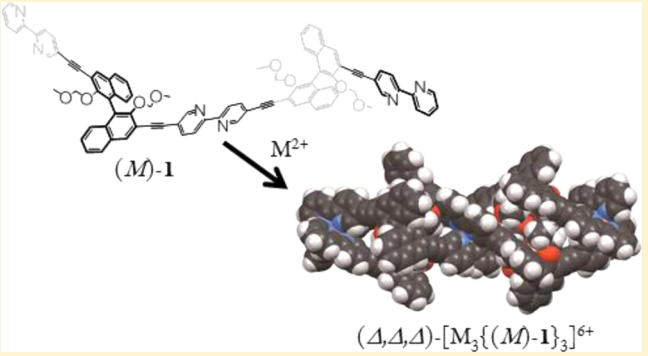

INTRODUCTION

Helices and spirals are virtually ubiquitous, and their simply aesthetically appealing structure has fascinated humans for a long time and has caused the use of this motif in numerous examples in architecture and arts. However, helical structures are not only found in macroscopic objects but are also well-known motifs in (supra-)molecular sciences as for instance the DNA double helix. Metallosupramolecular helicates represent another archetype of such aggregates that have interesting properties and can be used to study all kinds of self-processes like self-assembly and self-sorting in the sense of self-recognition and self-discrimination.[1] Another important aspect is that they are inherently chiral supramolecular objects,[2] and the mechanical coupling of two or more metal binding sites in a single ligand strand offers an outstanding opportunity to control the relative stereochemistry of stereogenic metal centers which is difficult to achieve otherwise.[2−4] Almost all of the studies concerning the diastereoselective formation of helicates have been done with dinuclear complexes so far,[5] and these processes are already challenging since an enantiomerically pure ligand can in principle give rise to three different diastereomeric dinuclear complexes, whereas a racemic ligand can even form up to nine stereoisomeric double-stranded and 12 stereoisomeric triple-stranded dinuclear helicates.

In 2002, we made our first contribution to this field when we reported on the synthesis of an enantiomerically pure C_2-symmetrical bis(bipyridine) 2,2′-dihydroxy-1,1′-binaphthyl (BINOL) ligand and its completely diastereoselective self-assembly of dinuclear helicates upon coordination to late transition metal ions.[6] Since then, we were able to extend our studies to a number of other dissymmetric ligands based on Tröger's base derivatives,[7] D-isomannide,[8] further BINOL derivatives,[9] and 9,9′-spirobifluorene derivatives,[10] thereby gaining a deeper understanding of the scope and limitations of our concept.[11] However, we have also been restricted to the formation of dinuclear helicates so far. To take our approach a step further, we present the synthesis of tris(bipyridine) ligand

Received: June 26, 2014
Published: July 22, 2014

dx.doi.org/10.1021/ja506327c | J. Am. Chem. Soc. 2014, 136, 11830−11838

1 in two enantiomeric forms here that has two BINOL groups as stereogenic elements and is designed for the formation of double- and triple-stranded trinuclear helical coordination compounds. Such higher nuclear complexes are much more challenging since the number of stereoisomers rises even more.

RESULTS AND DISCUSSION

Synthesis. (*P*,*P*)-**1** and (*M*,*M*)-**1** could each be prepared in a convergent 13-step synthesis outlined in Schemes 1 and 2.

Scheme 1. Synthesis of Monoethynylated BINOL Derivative 5

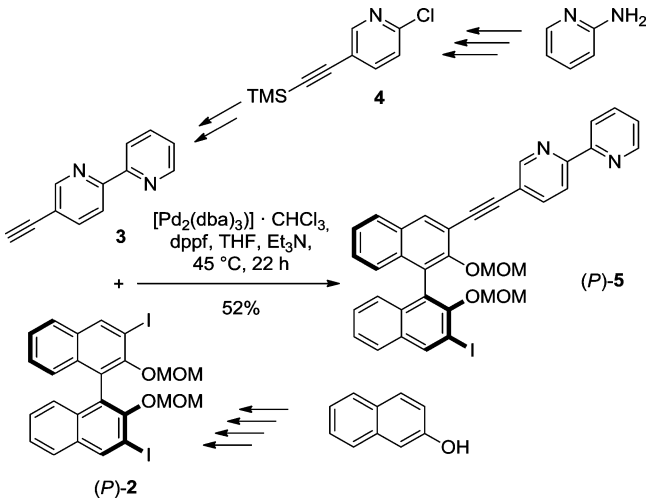

Scheme 2. Synthesis of Tris(bipyridine) Ligand 1

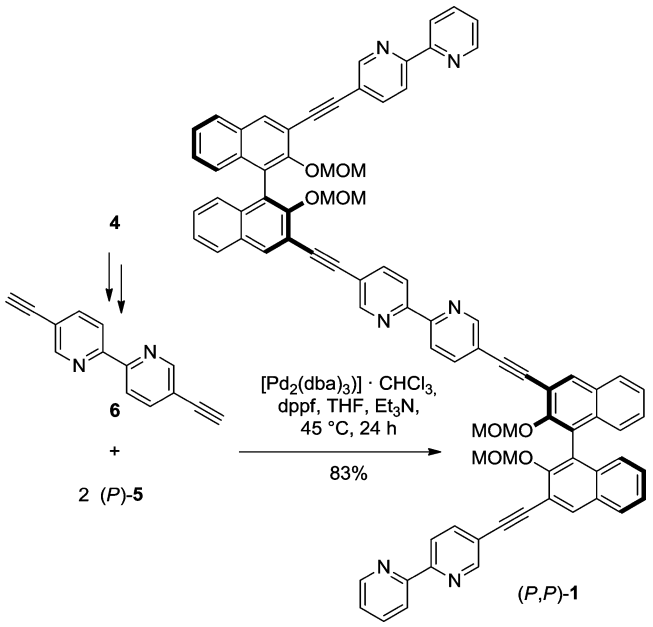

Both enantiomers of 3,3′-diiodo-2,2′-(methoxymethoxy)-1,1′-binaphthyl ((*P*)- and (*M*)-**2**) were synthesized in four steps from 2-naphthol following known procedures.[12−14] The cross-coupling partner 5-ethynyl-2,2′-bipyridine (**3**) was prepared in five steps from 2-aminopyridine involving an electrophilic iodination followed by a Sandmeyer-like chlorination to 2-chloro-5-iodopyridine and a first Sonogashira reaction with (trimethylsilyl)acetylene, leading to 2-chloro-5-{(trimethylsilyl)ethynyl}pyridine (**4**).[15] **4** was subjected to a Negishi cross-coupling with 2-bromopyridine, and cleavage of the silyl protecting group finally gave **3**.[16] Reaction of **2** and **3** in a single Sonogashira cross-coupling reaction afforded monoethynylated BINOL derivative **5** (Scheme 1).

Bis(ethynylated) 2,2′-bipyridine **6** (Scheme 2) was synthesized in a palladium-catalyzed homocoupling reaction of **4** and subsequent deprotection of the alkyne functions.[17] Two-fold Sonogashira coupling of **6** with 2.1 equiv of (*P*)- or (*M*)-**5** finally furnished the desired (*P*,*P*)-**1** and (*M*,*M*)-**1**, respectively.

Coordination Studies: Structural Assignment. To generate helicates, we treated solutions of the enantiomerically pure ligands (*P*,*P*)- and (*M*,*M*)-**1** with solutions of late transition metal salts, resulting in the specific color changes expected for bipyridine complexes: silver(I), yellow; zinc(II), pale yellow; copper(I), red-brown; copper(II), green; and iron(II), dark red.

In order to verify the formation of discrete double-stranded or triple-stranded trinuclear coordination compounds and rule out oligomeric or polymeric species, we explored the stoichiometry of the metal complexes with ESI mass spectrometric methods.

The spectrum of the silver complex (Figure 1a) shows the most intense signal at *m*/*z* 978.2 that can be assigned to the expected double-stranded $[Ag_3\mathbf{1}_2]^{3+}$ ion assuming that each silver ion adopts a tetrahedral coordination by four bipyridine N atoms. Interestingly, two other signals with marked intensity can be observed at *m*/*z* 1413.4 and *m*/*z* 760.1. As the former

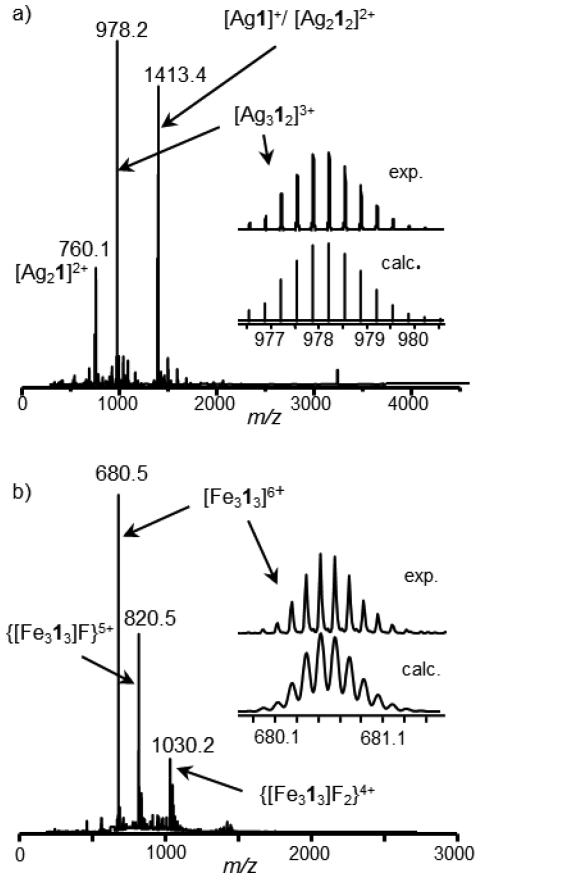

Figure 1. Positive ESI-MS spectra of 5×10^{-5} mol/L solutions of (a) $[Ag_3\mathbf{1}_2](BF_4)_3$ and (b) $[Fe_3\mathbf{1}_3](BF_4)_6$ in dichloromethane/acetonitrile (2:1).

dx.doi.org/10.1021/ja506327c | J. Am. Chem. Soc. 2014, 136, 11830−11838

one results from a mixture of two ions—a doubly charged species consisting of two metal ions and two ligands and a singly charged ion built up from one metal ion and one ligand strand—the latter one can be assigned to a doubly charged species with two metal ions being bound to a single ligand. Both of these are decomposition fragments of the intact double-stranded trinuclear assembly resulting from the ESI process as it has been observed for the silver complexes of other ligands before.[6−10] The spectra of freshly prepared copper(I) helicates are simpler to interpret since the copper complexes' tendency to undergo fragmentation is obviously much lower than the one of the silver ions. Hence, the most intense peak was found at m/z = 933.8, which can be assigned to the expected $[Cu_3\mathbf{1}_2]^{3+}$ ion. However, the copper(I) complexes were found to be surprisingly sensitive to oxidation, and thus, we also detected a mixed-valent complex containing two copper(I) and one copper(II) ion almost immediately. Obviously, the copper(II)-containing species are much more stable since we also obtained intense signals of oxidized triple-stranded complexes containing two or three copper(II) ions such as m/z = 684.3 and m/z = 821.3 that correspond to $[Cu_3\mathbf{1}_3]^{6+}$ and $[Cu_3\mathbf{1}_3]^{5+}$ ions, respectively (see Supporting Information) after 18 h, and we will come back to this at the end of this article.

The spectra of the corresponding zinc(II) (see Supporting Information) and iron(II) complexes (Figure 1b) are even easier to interpret. Both ions usually prefer an octahedral coordination geometry established by three chelating 2,2′-bipyridines. Thus, they were expected to form triple-stranded trinuclear coordination compounds with **1** which were indeed found to be the only species present in the solutions. The spectrum of the iron complex, for example, contains only signals of ions that can be assigned to intact trinuclear helicates that carry different numbers of counterions: a signal for a six-fold charged ion at m/z 680.5 resulting from $[Fe_3\mathbf{1}_3]^{6+}$, one for a five-fold charged ion at m/z 820.5 arising from $\{[Fe_3\mathbf{1}_3]F\}^{5+}$, and finally a quadruply charged ion giving rise to a signal at m/z 1030.2 that can be assigned as $\{[Fe_3\mathbf{1}_3]F_2\}^{4+}$.[18]

The successful formation of the desired discrete complexes is also indicated by the ^{1}H NMR spectra in 2:1 mixtures of dichloromethane-d_2/acetonitrile-d_3. The spectra of the zinc(II) and the silver(I) complexes show very distinct, sharp, and considerably shifted signals (Figure 2). Due to the presence of mixed-valent species containing copper(II) ions, the spectra of the copper complexes were only broad and hardly defined (see Supporting Information). The spectra of the equilibrated iron(II) complex show only rather broad signals which, however, is not due to the formation of oligomeric or polymeric species as the spectrum did not change upon dilution to a concentration of the complex of 8.5×10^{-5} mol/L (almost the concentration of the MS experiments, where we observed only the discrete trinuclear species). Hence, there might be two reasons for the signal broadening: either the dynamics of the ligand exchange in this solvent mixture is in the regime that would cause signal broadening or there might be an equilibrium between low- and high-spin iron(II) complexes that causes this phenomenon. This is in accordance with our earlier findings with other dinuclear iron(II) helicates.[6−9] Unfortunately, the dynamic behavior could not be slowed down enough to obtain a sharp set of signals due to precipitation of the compound upon cooling to lower temperatures. Changing the solvent to a 2:1 mixture of dichloromethane-d_2/DMSO-d_6, however, slowed down the self-assembly process considerably

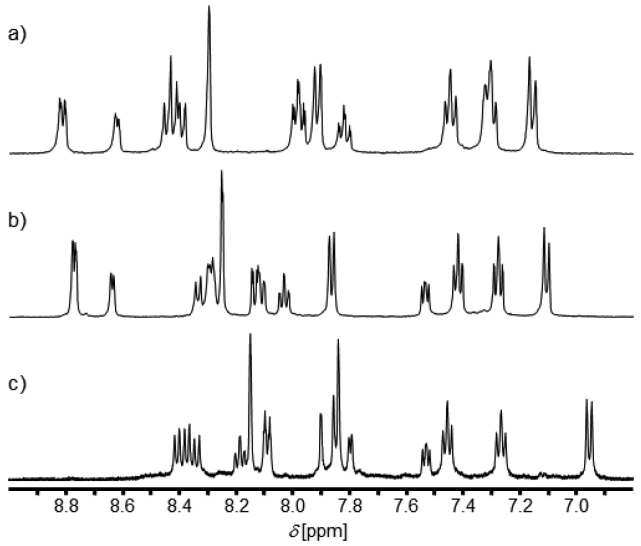

Figure 2. Aromatic region of the ^{1}H NMR spectra of (a) **1** (3.8×10^{-3} mol/L), (b) $[Ag_3\mathbf{1}_2](BF_4)_3$ (1.9×10^{-3} mol/L), and (c) $[Zn_3\mathbf{1}_3](BF_4)_6$ (1.28×10^{-3} mol/L) in dichloromethane-d_2/acetonitrile-d_3 (2:1).

as we had observed earlier for the self-assembly of some dinuclear iron(II) helicates.[9a] Under these conditions, again sharp and significantly shifted signals were observed that also prove that the iron salt is not contaminated by paramagnetic iron(III) ions, which could have been another reason for the signal broadening. However, the dynamics of the self-assembly process in this medium is so slow that one can observe the intermediate formation of several species until finally almost only a single product remains (see Supporting Information). Nevertheless, it should be noted that the broadening of the signals in the 2:1 mixture of dichloromethane-d_2/acetonitrile-d_3 might still be a result of a potential spin-crossover equilibrium since such processes are often also solvent-dependent.

Furthermore, these simple ^{1}H NMR spectra also reveal much about the stereoselectivity of the self-assembly process: in principle, six different diastereoisomers can be formed when an enantiomerically pure ligand is used since the metal centers are all stereogenic centers that can have (Δ,Δ,Δ)-, (Λ,Λ,Λ)-, (Λ,Δ,Λ)-, (Δ,Λ,Δ)-, (Δ,Δ,Λ)-, or (Λ,Λ,Δ)-configuration. A look at the spectra, however, reveals that obviously only a single one of these is actually formed because we only see one set of sharp signals and one would expect to see more if a mixture of diastereomers would be present. Therefore, the self-assembly process is (almost) completely diastereoselective for both double- and triple-stranded helicates. Furthermore, since the number of signals of the trinuclear coordination compounds is the same as the one observed for the free ligand, we can conclude that the assemblies have to be D_2- or D_3-symmetric because, only in these, the two halves of a single ligand strand stay magnetically equivalent. Thus, we can exclude the less symmetrical C_2- or C_3-symmetric (Δ,Δ,Λ)- and (Λ,Λ,Δ)-stereoisomers in which the two halves of a single ligand strand would be magnetically inequivalent.

To discern between these diastereomers in solution, one can apply NMR spectroscopic techniques. However, ROESY NMR experiments unfortunately did not allow a truly unambiguous assignment of the relative stereochemical arrangement of the bipyridine units with regard to the BINOL groups because we observed only very small ROE signals due to the long distances

dx.doi.org/10.1021/ja506327c | J. Am. Chem. Soc. 2014, 136, 11830−11838

between the respective protons, thus, preventing us from making an assignment. We therefore turned to circular dichroism (CD) spectroscopy to get further insight into the stereochemical properties of our complexes. Figure 3 depicts examples of the spectra of different complex solutions.

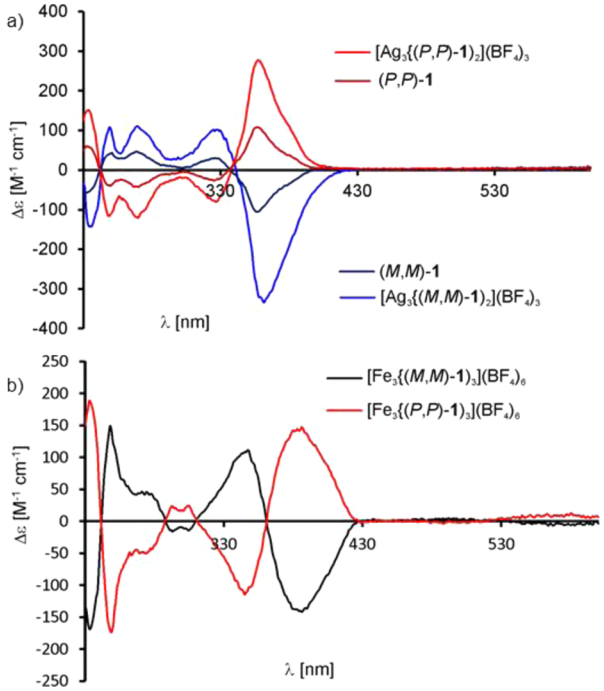

Figure 3. CD spectra of (a) free ligand **1** and its trinuclear silver(I) complexes and (b) its trinuclear iron(II) complexes. The spectra were measured in CH_2Cl_2/CH_3CN 1:1 at a concentration of 5×10^{-5} mol/L in a 1 mm cuvette.

The spectra of the free ligand and the silver(I) complexes do look very similar. This can be explained by the fact that the 2,2′-bipyridines adopt an almost perpendicular orientation to each other in the double-stranded helicates with the tetrahedral coordinated silver(I) centers. Thus, the opposite Cotton effects of the ligand-centered transitions cancel each other if the angle between the dipoles of the ligands is 90° due to the exciton theory.[19] Hence, CD spectroscopy alone is no help in elucidating the absolute stereochemistry of the stereogenic metal centers in this case just by analyzing the sign of the Cotton effects and/or comparison with literature data.[20−22]

The triple-stranded zinc(II), copper(II), and iron(II) complexes, however, give rise to very distinct CD spectra that are similar to each other but differ considerably from the ones of the free ligands. Again, the two enantiomers of **1** assemble into enantiomeric helicates. This indicates that the iron(II), the copper(II), and the zinc(II) complexes should have the same configuration. Furthermore, the spectra of the iron(II) and the copper(I) complexes do show MLCT bands at longer wavelengths (>530 nm). Thus, these spectra should in principle allow the assignment of the assemblies' absolute stereochemistry based on comparison with literature data.[20−22] Since the individual metal centers within our helicates do not necessarily have to have the same configuration, however, this approach is simply not feasible because the spectra are too complex to make an unambiguous assignment.

Therefore, theoretical calculations were performed for these helicates to identify the energetically preferred diastereomers and to simulate their spectra for comparison with the experimental ones (see Supporting Information for details) to make a reliable stereochemical assignment. These calculations are truly challenging since the cationic triple-stranded helicates, for example, contain 483 atoms and the task is to distinguish between diastereomers rather than enantiomers. Nevertheless, we optimized the structures of the (Δ,Δ,Δ)-, (Λ,Λ,Λ)-, (Λ,Δ,Λ)-, and (Δ,Λ,Δ)-configured trinuclear double-stranded copper(I) and triple-stranded zinc(II) helicates of the (*M*,*M*)-configured ligand at the DFT level using the dispersion-corrected TPSS[23]-D3[24] functional and the def2-SVP[25] basis set. The optimizations are performed with the TURBOMOLE suite[26] and applying the COSMO solvation model (CH_2Cl_2, $\varepsilon = 8.93$)[27] using the density fitting RI-J approach[28] to accelerate the geometry optimization. We refer to this level of computation as TPSS-D3/def2-SVP. In both cases, the (Λ,Λ,Λ)-configured helicates are found to be by far the most stable diastereomers, and the lowest energy conformers are shown in Figure 4. The (Δ,Λ,Δ)-configured helicates turn out

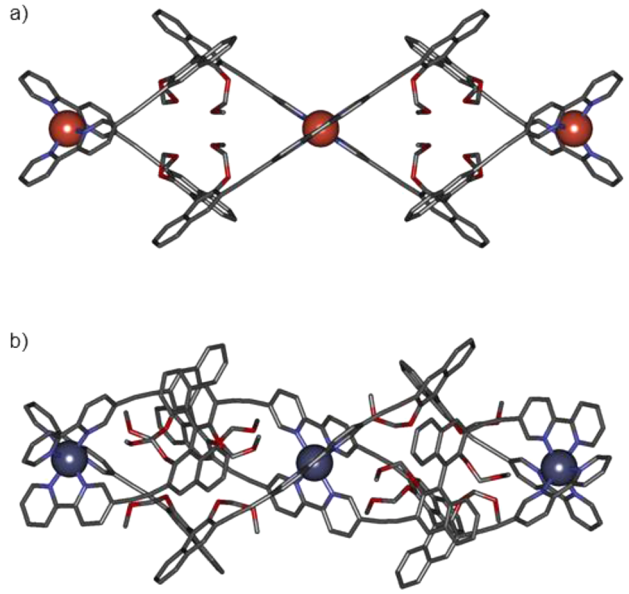

Figure 4. DFT-optimized structures (TPSS-D3/def2-SVP + COSMO (CH_2Cl_2)) of the most stable D_2- and C_2- (pseudo-D_3)-symmetric diastereomers of (a) double-stranded $[(\Lambda,\Lambda,\Lambda)\text{-}Cu_3\{(M,M)\text{-}\mathbf{1}\}_2]^{3+}$ and (b) triple-stranded $[(\Lambda,\Lambda,\Lambda)\text{-}Zn_3\{(M,M)\text{-}\mathbf{1}\}_3]^{6+}$ (hydrogen atoms are omitted for clarity).

to be the second stable diastereomers in both cases, which are about 26 and 43 kcal/mol higher in energy in the cases of copper(I) and zinc(II) helicates, respectively (see Supporting Information). These calculations strongly suggest that the (Λ,Λ,Λ)-helicate is the only thermodynamically preferred diastereomer when the (*M*,*M*)-configured ligands are used in our thermodynamically controlled self-assembly processes.

During these calculations, it turned out that the orientation of the MOM groups has a marked influence on the dihedral angles of the naphthyl groups of the binaphthyl units and, hence, on the overall structure of the helicate and its stability. The MOM groups can adopt several orientations (inward, mixed, and outward) in the quite open double-stranded copper(I) helicate, which results in three conformers (**a**, **b**, and **c**, respectively) of similar energy ($\Delta\Delta E < 5$ kcal/mol) but rather different overall structure with marked differences in the

dx.doi.org/10.1021/ja506327c | J. Am. Chem. Soc. 2014, 136, 11830−11838

metal−metal distances (see Supporting Information). The relatively flexible double-stranded copper(I) helicate prefers the conformation with *inward* oriented MOM side chains and with large BINOL dihedral angle (~103°) and thus long copper−copper distance. In the sterically more congested triple-stranded zinc(II) helicates, the calculations suggest that the confinement of the cavities forces the MOM groups to adopt an outward directed orientation together with smaller BINOL dihedral angle which is much more stable (approximately 16 kcal/mol) than the next best conformer.

Next, we performed time-dependent DFT calculations using a simplified Tamm−Dancoff approximation (sTDA)[29] together with the hybrid BHLYP[30] functional and the def2-SVP basis set[25] to model the CD spectra of various diastereomers of both the $[Cu_3\{(M,M)\text{-}\mathbf{1}\}_2]^{3+}$ and the $[Zn_3\{(M,M)\text{-}\mathbf{1}\}_3]^{6+}$ ions (see Supporting Information for details). These complexes contain 323 and 483 atoms, respectively, and, hence, represent very large systems for reliable first-principles modeling especially since hundreds of electronic excitations are required to simulate over the entire energy range in order to differentiate between diastereomers rather than enantiomers. Even though the huge size of the molecules forced us to make certain approximations in the DFT treatments (see Supporting Information), the calculated spectra of the (Λ,Λ,Λ)-diastereomers using the simplified Tamm−Dancoff approximation to time-dependent DFT (sTDADFT)[29] are for both ions in very good agreement with the experimental ones both in terms of position and absolute intensity of the individual bands and successfully reproduce nearly all experimentally observed bands in the broad low-energy range up to 240 nm (see Figure 5 and Supporting Information for a thorough discussion also of geometry and conformational effects and UV/CD spectra). The deviations of the band positions are systematic and acceptable concerning the size and complexity of the aggregates. Together with our recent study on even larger oligonuclear metallo-supramolecular palladium(II) complexes,[31] these sTDADFT calculations set new standards in the field of theoretical CD spectroscopy.

In the case of the relatively more flexible $[(\Lambda,\Lambda,\Lambda)\text{-}Cu_3\{(M,M)\text{-}\mathbf{1}\}_2]^{3+}$ diastereomer, several low-lying conformers are possible. Interestingly, the conformer **c** with the shortest Cu···Cu distance of about 8.8 Å due to a much smaller binaphthyl dihedral angle shows about 1.5-fold stronger CD peaks than the lowest conformer **a** with a considerably longer Cu−Cu distance of about 15.6 Å due to a larger binaphthyl dihedral angle, dependent on the MOM side chain orientation. In addition to relative energies of various diastereomers, the computed CD spectra provide clear proof for the (Λ,Λ,Λ)-configuration of both the double- and the triple-stranded helicates when the (*M*,*M*)-**1** ligand is used for the self-assembly of the trinuclear helicates.

Finally, we were also able to corroborate this stereochemical assignment of our helicates by an X-ray diffraction analysis of single crystals of the trinuclear triple-stranded copper(II) helicate of (*P*,*P*)-**1** which we obtained upon slow diffusion of tetrahydropyrane into a solution of the copper(II) helicate in a 3:1 mixture of dichloromethane/acetonitrile. The structure shown in Figure 6 nicely confirms the (Δ,Δ,Δ)-configuration of the three metal centers when the (*P*,*P*)-configured ligand **1** was used in the self-assembly of the helicate. Within this helicate, the copper(II) ions are found in a distorted octahedral 4 + 2 coordination sphere where four of the Cu−N coordinative bond lengths are between 2.01 and 2.07 Å and

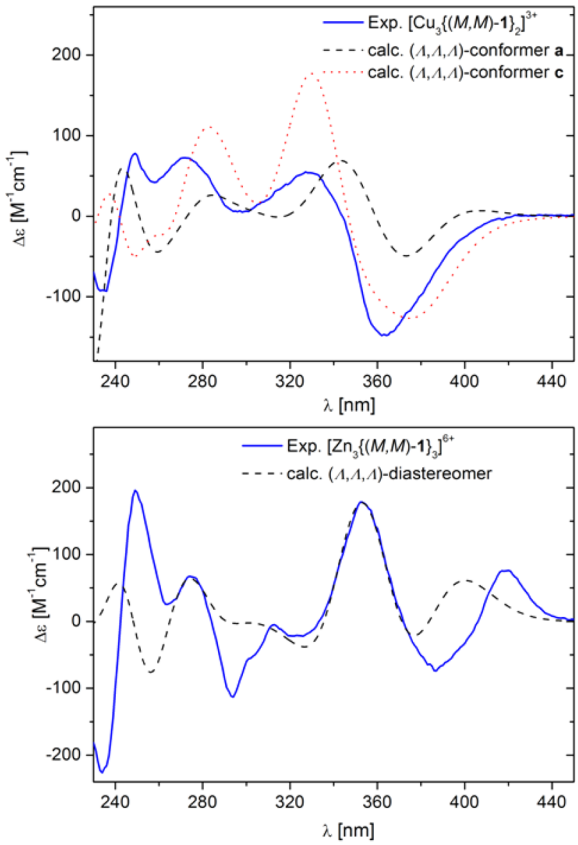

Figure 5. Experimental and calculated CD spectra (see Supporting Information for details) of $[(\Lambda,\Lambda,\Lambda)\text{-}Cu_3\{(M,M)\text{-}\mathbf{1}\}_2]^{3+}$ (top) and $([(\Lambda,\Lambda,\Lambda)\text{-}Zn_3\{(M,M)\text{-}\mathbf{1}\}_3]^{6+}$ (bottom).

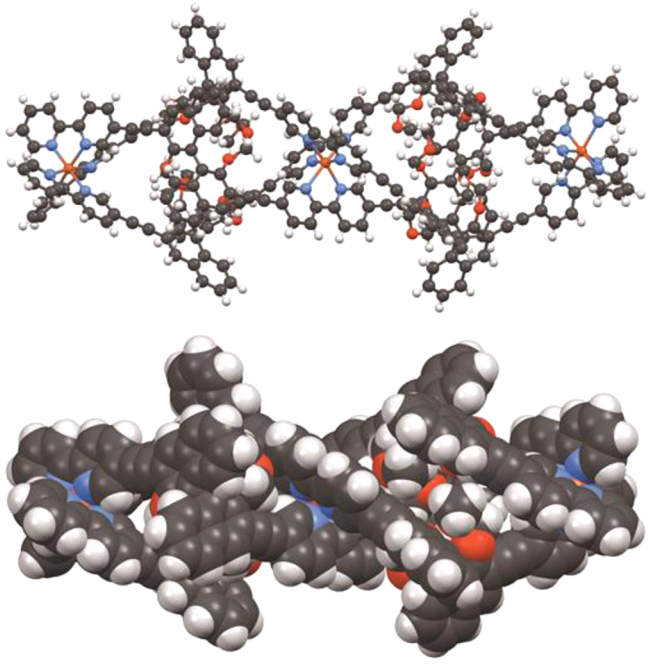

Figure 6. Structure of the triple-stranded trinuclear helicate $[(\Delta,\Delta,\Delta)\text{-}Cu_3\{(P,P)\text{-}\mathbf{1}\}_3](BF_4)_6$ as determined by X-ray diffraction analysis (counterions and solvent molecules are omitted for clarity, color code: red-brown, copper; gray, carbon; blue, nitrogen; red, oxygen; white, hydrogen).

dx.doi.org/10.1021/ja506327c | J. Am. Chem. Soc. 2014, 136, 11830−11838

the two others are considerably elongated, 2.22−2.40 Å (see Supporting Information).

In order to examine the chiral self-sorting[32] behavior of ligand **1**, we also performed experiments with a racemic mixture of (*M*,*M*)- and (*P*,*P*)-**1** with silver(I) and zinc(II) ions. In these cases, the number of potentially formed stereoisomers is much higher because one can think of 18 different stereoisomeric trinuclear double-stranded helicates and even 24 different stereoisomers of a trinuclear triple-stranded helicate that can in principle form from a racemic ligand. However, the self-assembly processes still proceeded completely diastereoselectively giving rise to the racemic pairs of the double- and triple-stranded homochiral diastereomers, respectively, that we had observed with the enantiomerically pure ligand. Hence, the self-assembly process proceeded in a narcissistic self-recognition manner. Following the classification of Schalley[33] and Schmittel,[34] this kind of a self-sorting process would be nonintegrative and $2^{5,5}$-fold (3) or $2^{6,6}$-fold (3) completive.[35] According to the algorithm of Schmittel, the degree of self-sorting $M = P/P_0$ in which P_0 is the number of all possible aggregates (in our case 18 or 24, respectively), and P is the number of the actually observed assemblies (in our case two), can be calculated as $M = 9$ for the double-stranded helicate and $M = 12$ for the triple-stranded helicate which is an extraordinary high value that proves the power of this approach to achieve diastereoselective self-assembly via self-sorting.

Redox Properties of Copper Helicates. Copper is exciting in the sense that it obviously prefers to form double-stranded helicates with ligand **1** in the oxidation state +I but triple-stranded ones in the oxidation state +II. This is in contrast to the behavior of another dinuclear helicate that was recently reported by Fabbrizzi and co-workers who found that the helicates stay double-stranded upon changing the oxidation state of the copper due to additional interligand interactions that stabilize the double-stranded structure.[36] However, such stabilizing interligand interactions are not present in our case, and hence, we observe a different behavior. As mentioned above, the brown-reddish solutions of copper(I) complexes of **1** in the usual millimolar concentration range used for the NMR spectroscopic measurements under ambient air were found to be surprisingly prone to oxidation converting the metal complexes into the corresponding copper(II) species of typical green color within 18 h (and a precipitate of an unknown copper species). Interestingly, this has not been observed with the bis(bipyridine) BINOL ligand studied before,[6] and we wanted to study this phenomenon further to elucidate the individual steps of this transformation that obviously contains three oxidation steps and at least one intermolecular step as one additional ligand has to be coordinated by the three metal centers. In particular, we were interested to see how many copper ions have to be oxidized before the double-stranded helicate transforms into a triple-stranded one upon addition of another ligand in order to stabilize the copper(II) centers.

Therefore, we first recorded a cyclic voltammogram which showed three distinct oxidation steps starting from the double-stranded trinuclear copper(I) helicate (see Supporting Information). When we then tried to reduce the triply oxidized species; however, we only found a single reduction and the whole process was not reversible (see Supporting Information). This indicates that the irreversible step occurs at the stage of a species containing two copper(II) and one copper(I) ion but does not tell anything about the stoichiometry of the intermediates. Hence, we thought to couple an electrochemical cell to a mass spectrometer to get an idea about the composition of the intermediates. However, again the reduction of the preformed trinuclear copper(II) helicate was impossible and precipitation during the oxidation of the trinuclear copper(I) helicate caused plugging of the ESI sources' cannula, thus making the measurements impossible.

However, mass spectrometry still proved to be the method of choice to study this phenomenon. In order to find out how many copper ions are oxidized before the addition of the third ligand, we diluted a freshly prepared solution of a double-stranded trinuclear copper(I) helicate to micromolar concentration to slow down the intermolecular and most likely rate-determining step. This turned out to be successful since we could still detect considerable amounts of the initial double-stranded trinuclear copper(I) helicate $[Cu(I)_3(\mathbf{1})_2]^{3+}$ in addition to some completely oxidized triple-stranded trinuclear copper(II) complexes $[Cu(II)_3(\mathbf{1})_3]^{6+}$ after 18 h. Furthermore, we observed an ion that can be assigned to a mixed-valent double-stranded helicate that contains two copper(I) and one copper(II) ions.

When we examined higher concentrated solutions, we also observed a very fast oxidation of the first copper ion resulting in the mixed-valent double-stranded species described above. However, the oxidation cascade does not stop at this stage but rapidly proceeds to the thermodynamically most stable completely oxidized triple-stranded trinuclear copper(II) helicate, and we were only able to detect a $[Cu(II)_2Cu(I)(\mathbf{1})_3]^{5+}$ ion as another intermediate.

Next, we decided to have a closer look at the reduction pathway via electron capture dissociation (ECD) MS^n experiments[37] despite the fact that this technique has hardly been used for the characterization of mononuclear metal complexes[38] or even oligonuclear metallosupramolecular complexes so far.[39] Reasons for its rare use might be that it can only be applied to doubly and even higher charged cations and that the abundance of fragment ions are usually rather low compared to other fragmentation methods like collision-induced dissociation or infrared multiphoton dissociation. Nevertheless, it is a very promising technique that can provide valuable information about the structure and the intrinsic redox behavior of a compound in the gas phase. During ECD, ions trapped in a FTICR cell are irradiated with low-energy electrons to induce either fragmentation or reduction after electron uptake.

We typically started these experiments with an ESI mass spectrum containing the intact triple-stranded trinuclear copper(II) helicate in different charge states (Figure 7a). The $[Cu_3(\mathbf{1})_3]^{6+}$ ion was mass selected and subjected to a first ECD process. The resulting ECD MS/MS is shown in Figure 7b. Interestingly, we observed a rather intense signal arising from a $[Cu_3(\mathbf{1})_3]^{5+}$ ion, but we did not detect any five-fold positively charged fragment $[Cu_3(\mathbf{1})_2]^{5+}$ that had lost a ligand. Hence, we conclude that a double-stranded helicate containing two copper(II) ions is just not stable, whereas a triple-stranded complex with one supposedly reduced copper center is.

Fortunately, the intensity of this $[Cu_3(\mathbf{1})_3]^{5+}$ ion was large enough to even perform an ECD/ECD MS^3 experiment, and the resulting spectrum is shown in Figure 7c. Clearly, the second ECD process does not result in a stable $[Cu_3(\mathbf{1})_3]^{4+}$ that would formally represent a complex containing one copper(II) ion and two copper(I) ions. Instead, a charge-separating fragmentation is observed which leads to the double-stranded triply charged Cu(I) helicate $[Cu_3(\mathbf{1})_2]^{3+}$ and a copper-free monocationic ligand which has lost a MOM group.

dx.doi.org/10.1021/ja506327c | J. Am. Chem. Soc. 2014, 136, 11830−11838

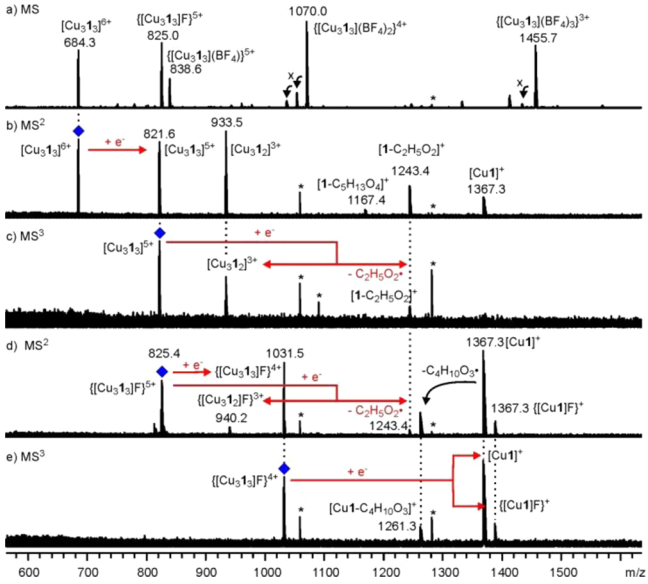

Figure 7. ECD-FTICR mass spectrometric studies on the triple-stranded trinuclear copper(II) helicate: (a) positive ESI-MS of a 5 × 10^{-5} mol/L solution of $[Cu_3(\mathbf{1})_3](BF_4)_6$ in dichloromethane/acetonitrile 2:1, (b) ECD MS/MS of $[Cu_3(\mathbf{1})_3]^{6+}$, (c) ECD/ECD MS^3 of $[Cu_3(\mathbf{1})_3]^{5+}$, (d) ECD MS/MS of $[Cu_3(\mathbf{1})_3F]^{5+}$, (e) ECD/ECD MS^3 of $[Cu_3(\mathbf{1})_3F]^{4+}$. Arrows with × mark losses of BF_3; *, electronic noise. The blue rhombs mark the mass-selected ions in the MS^n experiments.

The formation of this ion can be rationalized by a two-step process: The neutral ligand is oxidized to a ligand radical cation, thus enabling the formation of the stable double-stranded helicate with three Cu(I) ions. The ligand radical cation then loses a MOM radical—a reasonable hypothesis in regard of the fact that this fragmentation usually dominates the EI spectra of MOM-protected BINOL ligands. Gas-phase one-electron reduction of the triple-stranded Cu(II) helicate without ligand loss is successfully achieved for the other charge states, as well (Figure 7d and Supporting Information). Again, it is the second electron uptake that induces fragmentation (Figure 7e): ECD of the mass-selected reduced helicate $\{[Cu_3(\mathbf{1})_3]F\}^{4+}$ leads to a disassembly into the mononuclear complexes $[Cu(\mathbf{1})]\}^+$ and $\{[Cu(\mathbf{1})]F\}^+$. In addition, the 5+ species with one fluoride anion shows some interesting ligand expulsion already after the first electron uptake (Figure 7d). Yet, the hypothetic quadruply charged double-stranded helicate with one Cu(I) and two Cu(II) ions $\{[Cu_3(\mathbf{1})_2]F\}^{4+}$ is not observed. Instead, the triply charged analogue $\{[Cu_3(\mathbf{1})_2]F\}^{3+}$ with two Cu(I) ions is formed. The additional electron stems from the expelled ligand detected as a cation that has lost a MOM group similar to the findings described above. This finding nicely corroborates the results obtained by the mass spectrometric experiments with the diluted solutions where we did not find any triple-stranded species containing only one copper(II) ion.

Combining these observations, we were able to obtain a reasonably detailed overview about the redox behavior of our copper helicates which is depicted in Scheme 3.

SUMMARY AND CONCLUSIONS

In summary, we have synthesized a dissymmetric tris(2,2′-bipyridine) ligand **1** in two enantiomerically pure forms containing two BINOL units as stereogenic elements. This ligand undergoes diastereoselective self-assembly to enantiomerically pure trinuclear helicates upon coordination to late transition metal ions as could be proven by a combination of ESI mass spectrometric, NMR and CD spectroscopic means, and X-ray diffraction. Silver(I) and copper(I) ions form double-stranded $[M_3(\mathbf{1})_2]^{3+}$ helicates where the distance of the two outer silver ions is about 3.1 nm, whereas the zinc(II), iron(II), and copper(II) ions all form the respective triple-stranded $[M_3(\mathbf{1})_3]^{6+}$ helicates with the two outer metal centers being about 3.0−3.4 nm apart from each other. In order to assign the stereochemistry of the stereogenic metal centers, we performed DFT calculations on these helicates. Despite the fact that these helicates contain up to 483 atoms, which forced us to apply some further approximations, in particular, regarding the size of the AO basis set, these calculations were still accurate enough to allow an unambiguous assignment via comparison of experimental and theoretically simulated CD spectra. These sTDADFT treatments involving thousands of orbitals and hundreds of excited states represent new standards in the field of theoretical electronic spectroscopy. Hence, we were able to deduce that (*M*,*M*)-configured ligand **1** gives rise to (Λ,Λ,Λ)-

Scheme 3. Redox Behavior of Trinuclear Copper Helicates Green, Ligand 1; Red Circles, Copper(II) Ions; Yellow Circles, Copper(I) Ions; Blue Frames Indicate that These Species could be Detected Experimentally[a]

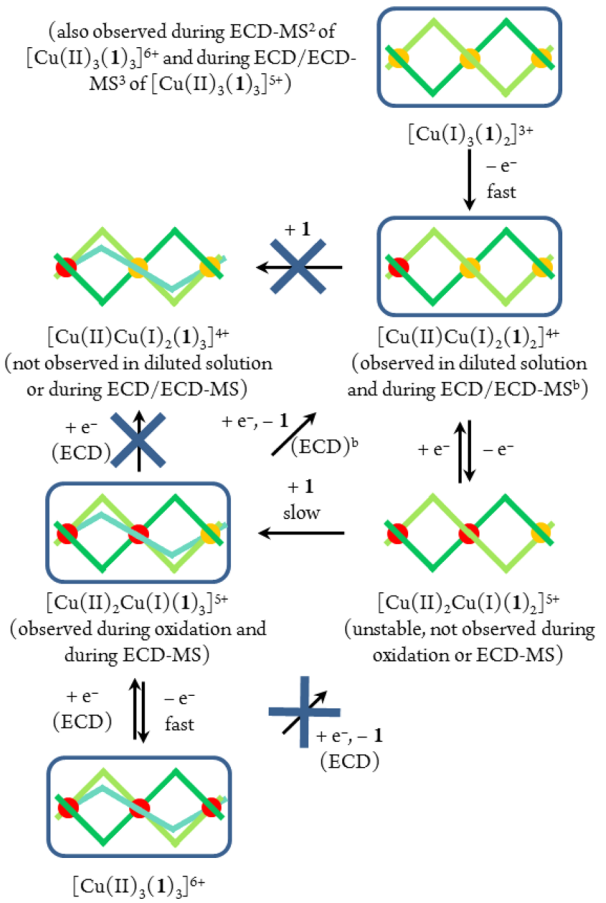

[a]Please note that we do not know the exact positions of the copper centers that are oxidized or reduced first, and hence, these cartoons are rather meant as visualization tools to distinguish between double- and triple-stranded as well as mixed-valent species. [b]The double-stranded helicate containing one copper(II) and two copper(I) ions was observed during ECD MS^2 of $\{[Cu(II)_2Cu(I)(\mathbf{1})_3]F\}^{5+}$ as an $\{[Cu(II)Cu(I)_2(\mathbf{1})_2]F\}^{3+}$ ion.

configured helicates, whereas (*P*,*P*)-**1** forms (Δ,Δ,Δ)-configured complexes independently of the metal ion used. This assignment was further confirmed by X-ray diffraction analysis of the trinuclear triple-stranded copper(II) helicate (Δ,Δ,Δ)-$[Cu_3\{(P,P)\text{-}\mathbf{1}\}](BF_4)_6$. According to the calculations, these two diastereomers are strongly preferred by as much as ca. 26 kcal/mol in the case of the double-stranded copper(I) helicate and even 43 kcal/mol in the case of the triple-stranded zinc(II) helicate, compared to the next stable diastereomers. Due to this large energetic difference of the possible diastereomers, the self-assembly of the helicates from racemic **1** proceeds in a completely narcissistic self-recognition manner whose degree of self-sorting *M* can be calculated to *M* = 9 for the double-stranded helicate and *M* = 12 for the triple-stranded helicate according to the algorithm of Schmittel. These are extraordinarily high values that prove the power and reliability of this approach to achieve high-fidelity diastereoselective self-assembly via chiral self-sorting that gives rise to stereochemically well-defined nanoscaled objects.

Interestingly, double-stranded copper(I) helicates of ligand **1** are readily oxidized to triple-stranded copper(II) helicates under ambient air. We were able to elucidate the sequence of the intermediate steps of this complex redox process that involves three redox steps and an addition/elimination of a ligand by recording ESI mass spectrometric experiments with copper(I) helicate solutions of very low concentration and by performing ECD/ECD-MS measurements starting from the fully oxidized triple-stranded copper(II) helicate. The latter technique has, in fact, been used for the first time here to follow the reduction of such metallosupramolecular assemblies and proves that this method can provide versatile information not only on the structure of a given (metallosupra-)molecular aggregate but also on its intrinsic redox properties.

■ ASSOCIATED CONTENT

Ⓢ Supporting Information

Synthetic procedures, characterization data, NMR spectra, details on computational studies, X-ray data, cyclic voltammetry, details on ECD MS studies. This material is available free of charge via the Internet at http://pubs.acs.org.

■ AUTHOR INFORMATION

Corresponding Authors

grimme@thch.uni-bonn.de
marianne.engeser@uni-bonn.de
arne.luetzen@uni-bonn.de

Notes

The authors declare no competing financial interest.

■ ACKNOWLEDGMENTS

Financial support from the Deutsche Forschungsgemeinschaft (SFB 813), the Academy of Finland (K.R. Grant Nos. 265328 and 263256), and the University of Jyväskylä is gratefully acknowledged. F.T. thanks the NGS-NANO, Finland, for a Ph.D. fellowship.

■ REFERENCES

(1) (a) Williams, A. *Chem.—Eur. J.* **1997**, *3*, 15. (b) Piguet, C.; Bernardinelli, G.; Hopfgartner, G. *Chem. Rev.* **1997**, *97*, 2005. (c) Albrecht, M. *Chem. Soc. Rev.* **1998**, *27*, 281. (d) Caulder, D. L.; Raymond, K. N. *Acc. Chem. Res.* **1999**, *32*, 975. (e) Albrecht, M. *Chem.—Eur. J.* **2000**, *6*, 3485. (f) Albrecht, M. *J. Inclusion Phenom. Macrocyclic Chem.* **2000**, *36*, 127. (g) Albrecht, M. *Chem. Rev.* **2001**, *101*, 3457. (h) Bünzli, J.-C. G.; Piguet, C. *Chem. Rev.* **2002**, *102*, 1897. (i) Mamula, O.; von Zelevsky, A. *Coord. Chem. Rev.* **2003**, *242*, 87. (j) Hannon, M. J.; Childs, L. J. *Supramol. Chem.* **2004**, *16*, 7. (k) Albrecht, M. *Top. Curr. Chem.* **2004**, *248*, 105. (l) Piguet, C.; Borkovec, M.; Hamkacek, J.; Zeckert, K. *Coord. Chem. Rev.* **2005**, *249*, 705. (m) He, C.; Zhao, Y.; Guo, D.; Lin, Z.; Duan, C. *Eur. J. Inorg. Chem.* **2007**, 3451. (n) Albrecht, M.; Fröhlich, R. *Bull. Chem. Soc. Jpn.* **2007**, *80*, 797. (o) Maayan, G., Albrech, M., Eds. *Metallofoldamers: Supramolecular Architectures from Helicates to Biomimetics*; Wiley: Chichester, UK, 2013.

(2) For an overview on different aspects of supramolecular chirality, see: Crego-Calama, M., Reinhoudt, D. N. *Top. Curr. Chem.* **2006**, *265*.

(3) Further reviews on diastereoselective self-assembly processes of metallosupramolecular aggregates: (a) Keene, F. R. *Chem. Soc. Rev.* **1998**, *27*, 185. (b) Telfer, S. G.; Kuroda, R. *Coord. Chem. Rev.* **2003**, *242*, 33. (c) Seeber, G.; Tiedemann, B. E. F.; Raymond, K. N. *Top. Curr. Chem.* **2006**, *265*, 147. (d) Lee, S. J.; Lin, W. *Acc. Chem. Res.* **2008**, *41*, 521.

(4) Some reviews and books on the stereoselective synthesis of coordination compounds: (a) von Zelewsky, A. *Stereoschemistry of Coordination Compounds*; Wiley: New York, 1996. (b) von Zelewsky, A. *Coord. Chem. Rev.* **1999**, *190−192*, 811. (c) Knof, U.; von Zelewsky, A. *Angew. Chem., Int. Ed.* **1999**, *38*, 302. (d) von Zelewsky, A.; Mamula, O. *J. Chem. Soc., Dalton Trans.* **2000**, 219. (e) Amouri, H.; Gruselle, M. *Chirality in Transition Metal Chemistry*; Wiley: New York, 2008.

(5) For a more comprehensive list of examples for diastereoselective self-assembly of helicates, see: Berg, M.; Lützen, A. Structural Aspects of Helicates. In *Metallofoldamers − Supramolecular Architectures from Helicates to Biomimetics*; Maayan, G., Albrech, M., Eds.; Wiley: Chichester, UK, 2013; p 125.

(6) Lützen, A.; Hapke, M.; Griep-Raming, J.; Haase, D.; Saak, W. *Angew. Chem., Int. Ed.* **2002**, *41*, 2086.

(7) (a) Kiehne, U.; Weilandt, T.; Lützen, A. *Org. Lett.* **2007**, *9*, 1283. (b) Kiehne, U.; Lützen, A. *Eur. J. Org. Chem.* **2007**, 5703. (c) Kiehne, U.; Weilandt, T.; Lützen, A. *Eur. J. Org. Chem.* **2008**, 2056. (d) Dalla Favera, N.; Kiehne, U.; Bunzen, J.; Hytteballe, S.; Lützen, A.; Piguet, C. *Angew. Chem., Int. Ed.* **2010**, *49*, 125.

(8) Kiehne, U.; Lützen, A. *Org. Lett.* **2007**, *9*, 5333.

(9) (a) Bunzen, J.; Bruhn, T.; Bringmann, G.; Lützen, A. *J. Am. Chem. Soc.* **2009**, *131*, 3621. (b) Bunzen, J.; Hovorka, R.; Lützen, A. *J. Org. Chem.* **2009**, *74*, 5228. (c) Bunzen, J.; Hapke, M.; Lützen, A. *Eur. J. Org. Chem.* **2009**, 3885. (d) Bunzen, J.; Kiehne, U.; Benkhäuser-Schunk, C.; Lützen, A. *Org. Lett.* **2009**, *11*, 4786.

(10) Piehler, T.; Lützen, A. *Z. Naturforsch. B* **2010**, *65b*, 329.

(11) Schalley, C. A.; Lützen, A.; Albrecht, M. *Chem.—Eur. J.* **2004**, *10*, 1072.

(12) Yang, X.-W.; Sheng, J.-H.; Da, C. S.; Wang, H.-S.; Su, W.; Wang, R.; Chan, A. S. C. *J. Org. Chem.* **2000**, *65*, 295.

(13) Bähr, A.; Droz, A. S.; Püntener, M.; Neidlein, U.; Anderson, S.; Seiler, P.; Diederich, F. *Helv. Chim. Acta* **1998**, *81*, 1931.

(14) Gütz, C.; Hovorka, R.; Schnakenburg, G.; Lützen, A. *Chem.—Eur. J.* **2013**, *19*, 10890.

(15) Baxter, P. W. *J. Org. Chem.* **2000**, *65*, 1257.

(16) Lützen, A.; Hapke, M. *Eur. J. Org. Chem.* **2002**, 2292.

(17) Lützen, A.; Hapke, M.; Meyer, S. *Synthesis* **2002**, 2289.

(18) Tetrafluoroborate ions are well-known to fragment in solution or under the conditions of ESI processes to form fluoride ions. Thus, sometimes signals were found which can be assigned to metallosupramolecular aggregates that contain fluoride ions as counterions.

(19) Berova, N.; Nakanishi, K.; Woody, P. W. *Circular Dichroism: Principles and Applications*; Wiley-VCH: Weinheim, Germany, 2000; Chapter 12, p 337.

(20) Ziegler, M.; von Zelewsky, A. *Coord. Chem. Rev.* **1998**, *177*, 257.

(21) Murner, H.; von Zelewsky, A.; Hopfgartner, G. *Inorg. Chim. Acta* **1998**, *271*, 36.

(22) Prabaharan, R.; Fletcher, N. C.; Nieuwenhuyzen, M. *J. Chem. Soc., Dalton Trans.* **2002**, 602.

(23) Tao, J. M.; Perdew, J. P.; Staroverov, V. N.; Scuseria, G. E. *Phys. Rev. Lett.* **2003**, *91*, 146401.

(24) (a) Grimme, S.; Ehrlich, S.; Krieg, H. *J. Chem. Phys.* **2010**, *132*, 154104. (b) Grimme, S.; Goerigk, L. *J. Comput. Chem.* **2011**, *32*, 1456.
(25) (a) Schäfer, A.; Horn, H.; Ahlrichs, R. *J. Chem. Phys.* **1992**, *97*, 2571. (b) Weigend, F.; Ahlrichs, R. *Phys. Chem. Chem. Phys.* **2005**, *7*, 3297.
(26) Ahlrichs, R.; Bär, M.; Häser, M.; Horn, H.; Kölmel, C. *Chem. Phys. Lett.* **1989**, *162*, 165; *TURBOMOLE* V6.5 2013, a development of University of Karlsruhe and Forschungszentrum Karlsruhe GmbH, 1989−2007, TURBOMOLE GmbH, since 2007; available from http://www.turbomole.com.
(27) Klamt, A.; Schüürmann, G. *J. Chem. Soc., Perkin Trans. 2* **1993**, 799.
(28) (a) Eichkorn, K.; Weigend, F.; Treutler, O.; Ahlrichs, R. *Theor. Chem. Acc.* **1997**, *97*, 119. (b) Deglmann, P.; May, K.; Furche, F.; Ahlrichs, R. *Chem. Phys. Lett.* **2004**, *384*, 103.
(29) Grimme, S. *J. Chem. Phys.* **2013**, *138*, 244104.
(30) (a) Becke, A. D. *Phys. Rev. A* **1988**, *38*, 3098. (b) Lee, C.; Yang, W.; Parr, R. G. *Phys. Rev. B* **1988**, *37*, 785.
(31) Gütz, C.; Hovorka, R.; Klein, C.; Jiang, Q.-Q.; Bannwarth, C.; Engeser, M.; Schmuck, C.; Assenmacher, W.; Mader, W.; Topić, F.; Rissanen, K.; Grimme, S.; Lützen, A. *Angew. Chem., Int. Ed.* **2014**, *53*, 1693.
(32) (a) Osowska, K.; Miljanić, O. Š. *Synlett* **2011**, 1643. (b) Safont-Sempere, M. M.; Fernández, G.; Würthner, F. *Chem. Rev.* **2011**, *111*, 5784. (c) Saha, M. L.; Schmittel, M. *Org. Biomol. Chem.* **2012**, *10*, 4651−4684.
(33) (a) Jiang, W.; Schalley, C. A. *Proc. Natl. Acad. Sci. U.S.A.* **2009**, *106*, 10425. (b) Jiang, W.; Winkler, H. D. F.; Schalley, C. A. *J. Am. Chem. Soc.* **2008**, *130*, 13852.
(34) Mahata, K.; Schmittel, M. *J. Am. Chem. Soc.* **2009**, *131*, 16544.
(35) In the term "*X*^{y}-fold (*z*) completive", X is the number of different assemblies that actually form, *y* is the number of particles the assembly consists of, and *z* is the number of different components.
(36) Boicchi, M.; Brega, V.; Ciarrocchi, C.; Fabbrizzi, L.; Pallavicini, P. *Inorg. Chem.* **2013**, *52*, 10643.
(37) (a) Zubarev, R. A.; Kelleher, N. L.; McLafferty, F. W. *J. Am. Chem. Soc.* **1998**, *120*, 3265. (b) Zubarev, R. A.; Horn, D. M.; Fridriksson, E. K.; Kelleher, N. L.; Kruger, N. A.; Lewis, M. A.; Carpenter, B. K.; McLafferty, F. W. *Anal. Chem.* **2000**, *72*, 563. (c) Cooper, H. J.; Hakansson, K.; Marshall, A. G. *Mass. Spectrom. Rev.* **2005**, *24*, 201.
(38) (a) James, P. F.; Perugini, M. A.; O'Hair, R. A. *Eur. J. Mass. Spectrom.* **2009**, *15*, 145. (b) Kaczorowska, M. A.; Cooper, H. J. *J. Am. Soc. Mass Spectrom.* **2009**, *20*, 674.
(39) (a) Kaczorowska, M. A.; Hotze, A. C. G.; Hannon, M. J.; Cooper, H. J. *J. Am. Soc. Mass Spectrom.* **2010**, *21*, 300. (b) Hovorka, R.; Engeser, M.; Lützen, A. *Int. J. Mass Spectrom.* **2013**, *354/355*, 152.